8TH EUROPEAN CONFERENCE FOR AERONAUTICS AND AEROSPACE SCIENCES (EUCASS)

DOI: 10.13009/EUCASS2019-770

Reconfigurable Nonlinear Controller Under Turbulence Flight Condition

Burak Ergöçmen⋆

⋆*Middle East Technical University*

Üniversiteler Mahallesi, Dumlupınar Bulvarı No:106800 Çankaya Ankara/TURKEY

ergocmen.burak@metu.edu.tr

Abstract

Generally, during severe turbulence, there are autopilot limitations for every type of aircraft. Besides, the undesirable effects of the turbulence such as g-force, have to be lessened. As a result, for any aircraft type, reconfigurable flight controller can be useful to prevent undesired effects of the turbulence. In this paper, a reconfigurable nonlinear controller which consists of State Dependent Riccati Equation (SDRE) and linear algorithm, is used to slow down control surface movement to decrease undesirable forces but at the same time, continue degraded tracking pilot commands. Besides, SDRE Kalman filter is used for Euler angles in the sensor.

1. Introduction

The weather directly affects the safety of the flight. So, extraordinary efforts are strived to avoid meteorological related accidents. However, these accidents continue to occur. The turbulence is the one cause for the meteorological related accidents and incidents.[1] First, normally, during the planning phase or during flight, turbulent areas in the atmosphere can be avoided by meteorological reports such as significant weather charts (SWC), pilot reports (PIREP), significant meteorological information (SIGMET). Secondly, detection for turbulence during flight is an ongoing study. For instance, tests for Long-range Light Detection and Ranging (LIDAR) is continued and one of the usages of this technology is turbulence detection.[2] Even though there is a detection of the turbulence, flight control law has to be reconfigured for turbulence condition. In addition, many aircraft have weather radars which have turbulence mode, but there are false indications and even they can not identify turbulent areas. For example, there is no indication of clear air turbulence (CAT). As a result, pilots and aircraft continue exposing to turbulence. The result of the turbulence can be harmful to the aircraft, flight crew or passengers. An abrupt and excessive g-force brings about structural damage to the aircraft structure and control surfaces.[3]

There are different areas for turbulence. These areas are friction layer, clouds, and clear air. In the friction layer, the flow of the air is getting deteriorated by the thermal and mechanical turbulence. In the clear air, near the tropopause, especially with the jet stream, there is clear air turbulence which causes the loss of control in flight (LOC-I) and the airframe damage. In the clouds, there is a turbulence condition but can be avoided by the usage of the weather radar.[4] The turbulence intensity is sub-divided as light, moderate, severe, and extreme.[3]

Firstly, to avoid these effects during turbulent conditions, various type of Airbus and Boeing aircraft have a load alleviation function. This function is used to reduce g-force on the wing with the help of the aileron and spoiler control surfaces. Normally, for this function, deflection of the aileron, spoiler or both is performed automatically. However, in this paper, the main objective is reducing unnecessary movement of the control surfaces to reduce g-force on the aircraft but at the same time tracking command continue to work with degraded function. In this work, this function is done without using g-force or gust measurements in the control law. Besides, this model does not have a spoiler. As a result, this paper is not focused on disturbance rejection.

Secondly, written in the aircraft cockpit reference handbook or pilot operating handbook, the pilot uses a turbulent penetration speed. In addition, generally for non fly-by-wire aircraft such as Beechcraft 350, the pilot disengages the autopilot altitude hold mode and flies the aircraft manually without chasing airspeed and altitude, keeps wing level and avoids using trim.[5] However, written in the Boeing 737 flight crew operating manual (FCOM), during a flight in light to moderate turbulence, the autopilot and/or autothrottle may remain engaged unless the performance is objectionable. In severe turbulence, pilot disengages autothrottle and change autopilot mode to control wheel steering (CWS) which means manually flown procedure but without disengaging the autopilot.[6] In Airbus A321 with fly-by-wire flight

controls, autopilot and auto-thrust are maintained to engaged as a checklist procedure as long as autopilot performance is acceptable.[7]

Thirdly, there is an autopilot mode on the autopilot panel or flight control system to soften autopilot response for chasing altitude during turbulence. Depending on the aircraft model, this mode is called turbulence (TURB), turbulence smoothing or soft ride. In this paper, this TURB mode is used for the autopilot.

In brief, the first rule for turbulence avoidance is using existing detection means such as reports or airborne weather radar (AWR). However, if unpredictable turbulence is encountered, depending on the aircraft type, following golden rules written in the flight crew operating manual (FCOM) or pilot operating handbook (POH) is the best action. Common golden rules are maintaining turbulence penetration speed and not to chase altitude or airspeed with or without autopilot depending on the aircraft.

As a result, if the autopilot can be reconfigurable, excessive forces on the aircraft body can be averted. Besides, unnecessary movement of the control surface to maintain altitude or speed can be prevented. This protection can be life-saving. In this work, the pilot or operator only activates turbulence (TURB) mode of the autopilot. After that, the flight controller is reconfigured to the degree of the turbulence with the help of turbulence detection (TD). In this work, turbulence detection is assumed to detect the severity of the turbulence.

Turbulence effects are studied during controller design. By Santos et al[8] SDRE control algorithm is used for elevator deflection to stabilize wing angle oscillation; by Ilif[9] identification and stochastic control is used under turbulence condition; by Steck et al[10] the reconfigured command filters are used for adaptive dynamic inverse flight controller and turbulence effects are studied; by Yang and Juan[11] adaptive cerebellar model articulation controller (CMAC) is used for landing aircraft safely during severe turbulence; by Jafar et al[12] dynamic output feedback robust controller is mixed with linear matrix inequality (LMI) approach to minimize the effect of turbulence conditions for the UAV; by Miyagaki and Suzuki[13] MPC is used for landing safely with the help of the LIDAR which measures air disturbance in the atmosphere.

In addition, in literature, gust load alleviation(GLA) and disturbance rejection are studied: by Wen et al[14] adaptive controller with a different gains is used for turbulence compensation; by Liu et al[15] a linear quadratic Gaussian (LQG) based MPC is used for GLA; by Sato[16] gust alleviation flight controller using robust Model Predictive Control (MPC) is introduced; by Aouf et al[17] $\mathcal{H}_2$ and $\mathcal{H}_\infty$ optimal controller is used to reduce the effects of the wind gust on the vertical acceleration as a GLA; by Giesseler et al[18] MPC is used for GLA; by Fonte et al[19] aeroelastic model is used for designing symmetric, active gust alleviation system for next generation regional transport aircraft, by Wang et al,[20] an Incremental Nonlinear Dynamic Inversion (INDI) controller is used for the flexible aircraft GLA problem.

In this paper, State Dependent Riccati Equation (SDRE) algorithm which is a nonlinear control algorithm in the modern control theory, is used for the autopilot. As a summary, in the reconfiguration mechanism, there are different Q and R weight matrices with respect to turbulence severity and altitude for the flight control computer (FCC). In the event of different turbulence condition which is assumed to be detected by the turbulence detection (TD), the pilot or operator only engages turbulence (TURB) mode. Depending on the detection of intensity of turbulence and the altitude, the reconfiguration mechanism sends different Q and R matrices for SDRE control algorithm.

This paper is organized as follows. In Section II, components of the simulation are introduced. In Section III, the SDRE control algorithm is developed for FCC. Besides, mathematical representation, inner and outer loops are given for the SDRE algorithm. In Section IV, the SDRE Kalman filter; in Section V, Dryden turbulence model is developed. In Section VI, the reconfiguration mechanism is explained with the help of the weight matrices. In Section VII and VIII, some simulation results and conclusions are presented.

2. The Components of the Simulation

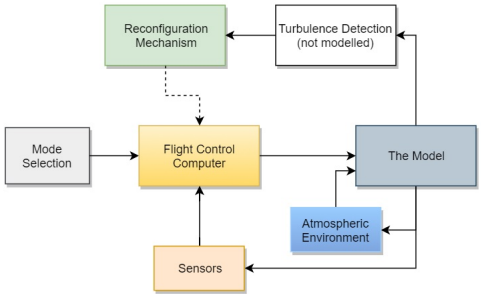

Figure 1: Models of the simulation.

The general architecture for simulation model in Matlab/Simulink is shown in Fig. 1. First of all, there is an aircraft model in the model block. It contains aerodynamics derivatives, engine and actuator models of the aircraft model. With the help of the atmospheric environment model, turbulence can be injected into the UAV model. Besides, the severity of the turbulence can be adjusted. The Dryden Wind Turbulence Model is used to create turbulence condition. The output of this model contains the turbulence velocities (u_g, v_g, w_g) and rates (p_g, q_g, r_g) with respect to body axis. After, these values are included in the aircraft velocity and rates. Turbulence detection (TD) block is assumed to detect turbulence severity and sends this condition to the reconfiguration mechanism (RM). RM block is used to reconfigure flight control computer (FCC) block. It sends different Q and R matrices to SDRE calculator in the FCC.

There is a mode selection (MS) depicted in Fig. 2, which is used by the pilot or operator to control the aircraft with different modes. These modes are altitude hold, heading, altitude change with flight level change or vertical speed and airspeed holder. There are command filters and rate limiters for these commands. Besides, turbulence (TURB) mode is attached for engaging or disengaging turbulence reconfiguration for the autopilot. If it is engaged, the reconfiguration mechanism is activated with this signal and turbulence reconfiguration begins.

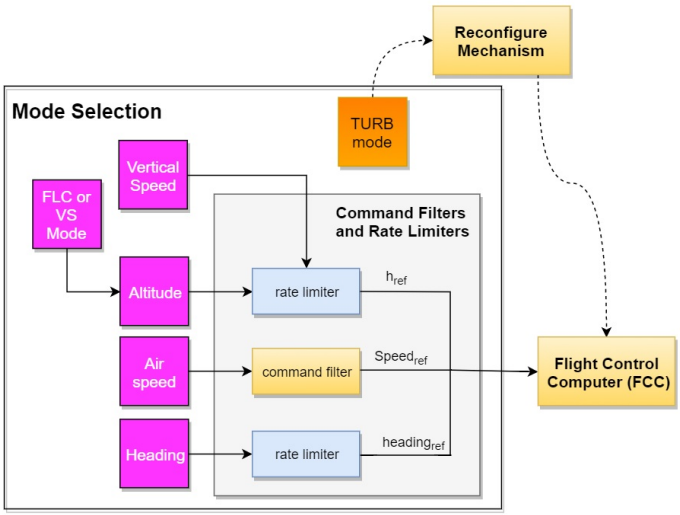

Figure 2: Mode selection (MS).

Table 1: Stability derivatives of the UAV in the stability axis.

	C_D	C_L	C_y	C_l	C_m	C_n
u	0.0312	-0.0059	-	-	-	-
α	0.1288	5.5776	-	-	-1.2005	-
β	-	-	-0.2006	-0.01534	-	0.06594
p	-	-	-0.0302	-0.5417	-	-0.0694
q	-	9.7010	-	-	-19.1029	-
r	-	-	0.1508	0.1197	-	-0.0462
δ_a	-	-	-	0.1189	-	0
δ_e	0.0446	0.5106	-	-	-1.7605	-
δ_r	-	-	0.0571	0.0019	-	-0.0202
	C_{D_o}	C_{L_o}	C_{y_o}	C_{l_o}	C_{m_o}	C_{n_o}
	0.0121	0.3515	0	0	0.0358	0

The 169 kg. UAV model is designed in an open source program, XFLR5. Aerodynamic derivatives depicted in Table 1, are obtained from XFLR5 in the stability axis. Aircraft parameters are set as: $m = 169kg$, $g = 9.8m/s^2$, $S = 2.1430m^2$, $c = 0.4680m$, $b = 4.7993m$, $I_{xx} = 60.34kg.m^3$, $I_{yy} = 66.92kg.m^3$, $I_{zz} = 126.90kg.m^3$, $I_{xz} = -3.299kg.m^3$. Control surface consists of elevator, aileron and rudder.

3. The Flight Control Computer

Flight control computer consists of reference commands block, SDRE calculator block and controller architecture depicted in Fig. 3. In the reference command block, adjusted altitude and heading are converted to respectively θ_{ref} and ϕ_{ref}. After that, this reference commands are transmitted to controller architecture. There are two loops (inner and outer) for the controller. The outer loop is used for controlling the Euler angles (ϕ and θ), the inner loop is for rates (p: roll rate, q: pitch rate, r: yaw rate). This signal (reference command signal) is multiplied by dynamically changing gains (SDRE-1 Tracker, SDRE-2 Tracker, and SDRE-2 Regulator). These gains are calculated in the SDRE calculator and feed the controller architecture. Before explaining the inner and the outer loop, the mathematical representation of the SDRE is given.

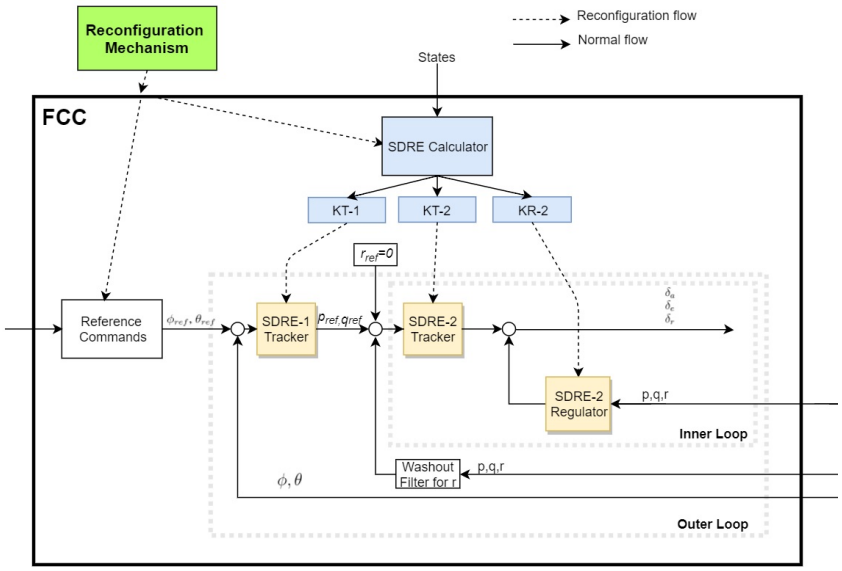

Figure 3: The SDRE controller.

3.1 The Mathematical Summary for SDRE Controller

In the flight control computer, SDRE algorithm is used. SDRE algorithm is a nonlinear control. It represents the dynamic of the system more accurate than the linear control techniques. First of all, nonlinear systems can be expressed as:

$$\dot{x}(t) = f(x) + B(x)u, x(0) = x_0 \tag{1}$$
$$y(t) = Cx(t) \tag{2}$$

The nonlinear term, **f(x)** can be transformed to **A(x)x**. A(x) and B(x) are state dependent coefficient (SDC) matrices which consists of states and updated by states. As a result, **A(x)** is constantly changing. Theoretically, there are infinite A(x) matrix created. The equation becomes:

$$\dot{x}(t) = A(x)x(t) + B(x)u(t) + f(t) \tag{3}$$
$$y(t) = Cx(t) \tag{4}$$

Some assumptions are made: The system is affine in the input, nonlinear in the state, autonomous and state observable. Also, f(t) is a nonlinear term which cannot be linearized. So, f(t) is not included in the A(x) matrix. At each instant, the matrix A is linear, so that the solution of the problem can be found by the linear quadratic optimal problem. One of the main objectives is minimizing quadratic performance index function or cost functional.[21] These functions are given for regulator and tracking problem:

$$J_R = \frac{1}{2}\int_0^\infty [x^T(t)Qx(t) + u^T(t)Ru(t)]dt \tag{5}$$

$$J_T = \frac{1}{2}\int_0^\infty [e^T(t)Qe(t) + u^T(t)Ru(t)]dt \tag{6}$$

x(t) is nth order state vector; **Q** is nxn order positive and symmetric semi-definite matrix (Q≥0); **R** is mxm order positive and symmetric definite matrix (R>0). Q and R are weight matrices and in this paper, they represented by **Q(a)** and **R(a)**, because they change with the **a** signal which comes from the reconfiguration mechanism.

For the regulator and tracking problems, algebraic Riccati equations (ARE) are given respectively:

$$PA(x) + A^T(x)P + Q - PBR^{-1}B^TP = 0 \tag{7}$$

$$PA(x) + A^T(x)P + C^TQC - PBR^{-1}B^TP = 0 \tag{8}$$

The tracking is represented as K_T and regulator is represented as K_R. The control law is calculated with the help of the P from algebraic Riccati equations. All control laws are given as:[22]

$$u(t) = -K_Rx(t) + K_Tz(t) \tag{9}$$

$$K_R = R^{-1}B^TP \tag{10}$$

$$K_T = R^{-1}B^T(PE - A^T)^{-1}W \tag{11}$$

$$E = BR^{-1}B^T \tag{12}$$

$$W = C^TQ \tag{13}$$

The mathematical representation of gains can be depicted as $K_T(P, A(x), B(x))$ and $K_R(P, B(x))$, because they vary. However, as a notation, these gains are given as K_{T-1}, K_{T-2}, and K_{R-2} for simplicity.

3.2 The Outer Loop

There are outer and inner loops for the SDRE controller architecture. In the outer loop the main objective is to control the θ_{ref} and ϕ_{ref}. In Eq. (14) states vector which consists of euler angles and in Eq. (15) input vector which consists of angular rates (respectively p:roll, q:pitch and r:yaw rate) are given for the outer loop. Therefore, A_1 is given in Eq. (16) and nonlinear like $B_1(x)$ SDC matrix is given in Eq. (17). Weight matrices, $Q_1(a)$ and $R_1(a)$, are given in Eq. (18) and Eq. (19). Finally, K_{T-1} are calculated with the help of A_1, $B_1(x)$, $Q_1(a)$, and $R_1(a)$ matrices.

$$x_1 = \begin{bmatrix} \phi & \theta & \psi \end{bmatrix}^T \tag{14}$$

$$u_1 = \begin{bmatrix} p & q & r \end{bmatrix}^T \tag{15}$$

$$\begin{bmatrix} \dot{\phi} \\ \dot{\theta} \\ \dot{\psi} \end{bmatrix} = \begin{bmatrix} 0 & 0 & 0 \\ 0 & 0 & 0 \\ 0 & 0 & 0 \end{bmatrix} \begin{bmatrix} \phi \\ \theta \\ \psi \end{bmatrix} + \tag{16}$$

$$\begin{bmatrix} 1 & \tan\theta\sin\phi & \tan\theta\cos\phi \\ 0 & \cos\phi & -\sin\phi \\ 0 & \frac{\sin\phi}{\cos\theta} & \frac{\cos\phi}{\cos\theta} \end{bmatrix} \begin{bmatrix} p \\ q \\ r \end{bmatrix} \tag{17}$$

$$Q_1(a) = diag(50, 50, 50) \tag{18}$$

$$R_1(a) = diag(0.8, 0.5, 0.6) \tag{19}$$

3.3 The Inner Loop

In the inner loop, the main objective is to control the p, q and r. In Eq. (20) states vector and in Eq. (21) input vector are given. δ_a, δ_e, δ_r are respectively aileron, elevator and rudder deflections in degree. However, throttle command (δ_t) is given by a separated controller which consists of proportional-integral-derivative. B_2 matrix and nonlinear like $A_2(x)$ SDC matrix are given in Eq. (22) and (23). Weight matrices, $Q_2(a)$ and $R_2(a)$, are given in Eq. (37) and Eq. (38). Finally, K_{T-2} and K_{R-2} are calculated with the help of $A_2(x)$, B_2, $Q_2(a)$, and $R_2(a)$ matrices.

$$x_2 = \begin{bmatrix} p & q & r \end{bmatrix}^T \tag{20}$$

$$u_2 = \begin{bmatrix} \delta_a & \delta_e & \delta_r \end{bmatrix}^T \tag{21}$$

$$\begin{bmatrix} \dot{u} \\ \dot{v} \\ \dot{w} \\ \dot{p} \\ \dot{q} \\ \dot{r} \end{bmatrix} = \begin{bmatrix} X_u & 0 & X_w & 0 & X_q - w & v \\ 0 & Y_v & 0 & Y_p + w & 0 & Y_r - u \\ Z_u & 0 & Z_w & -v & Z_q + u & 0 \\ 0 & I_1 I_{xx} L_v + I_2 I_{zz} N_v & 0 & a_{11} & a_{12} & a_{13} \\ M_u & 0 & M_w & a_{21} & a_{22} & a_{23} \\ 0 & I_2 I_{xx} L_v + I_5 I_{zz} N_v & 0 & a_{31} & a_{32} & a_{33} \end{bmatrix} \begin{bmatrix} u \\ v \\ w \\ p \\ q \\ r \end{bmatrix} + \tag{22}$$

$$\begin{bmatrix} 0 & X_{\delta_e} & 0 & X_{\delta_t} \\ Y_{\delta_a} & 0 & Y_{\delta_r} & 0 \\ 0 & Z_{\delta_e} & 0 & 0 \\ I_1 I_{xx} L_{\delta_a} + I_2 I_{zz} N_{\delta_a} & 0 & I_1 I_{xx} L_{\delta_r} + I_2 I_{zz} N_{\delta_r} & 0 \\ 0 & M_{\delta_e} & 0 & 0 \\ I_2 I_{xx} L_{\delta_a} + I_5 I_{zz} N_{\delta_a} & 0 & I_2 I_{xx} L_{\delta_r} + I_5 I_{zz} N_{\delta_r} & 0 \end{bmatrix} \begin{bmatrix} \delta_a \\ \delta_e \\ \delta_r \\ \delta_t \end{bmatrix} + \begin{bmatrix} -g \sin\theta \\ g \cos\theta \sin\phi \\ g \cos\theta \cos\phi \\ 0 \\ 0 \\ 0 \end{bmatrix} \tag{23}$$

$$a_{11} = I_1 I_{xx} L_p + I_2 I_{zz} N_p + I_4 q \tag{24}$$
$$a_{12} = 0 \tag{25}$$
$$a_{13} = I_1 I_{xx} L_r + I_2 I_{zz} N_r + I_3 q \tag{26}$$
$$a_{21} = -\frac{I_{xz}}{I_{yy}} p - \frac{I_7}{I_{yy}} r \tag{27}$$
$$a_{22} = M_q \tag{28}$$
$$a_{23} = \frac{I_{xz}}{I_{yy}} r \tag{29}$$
$$a_{31} = I_2 I_{xx} L_p + I_5 I_{zz} N_p + I_6 q \tag{30}$$
$$a_{32} = 0 \tag{31}$$
$$a_{33} = I_2 I_{xx} L_r + I_5 I_{zz} N_r - I_4 q \tag{32}$$

$$I_1 = \frac{I_{zz}}{I_8}, I_2 = \frac{I_{xz}}{I_8}, I_3 = \frac{(I_{yy} - I_{zz}) I_z z - I_{xz}^2}{I_8} \tag{33}$$
$$I_4 = \frac{(I_{xx} - I_{yy} + I_z z) I_{xz}}{I_8}, I_5 = \frac{I_{xx}}{I_8} \tag{34}$$
$$I_6 = \frac{(I_{xx} - I_{yy}) I_x x + I_{xz}^2}{I_8}, I_7 = I_{xx} - I_{zz} \tag{35}$$
$$I_8 = I_{xx} I_{zz} - I_{xz}^2 \tag{36}$$

$$Q_2(a) = diag(5, 5, 2) \tag{37}$$

$$R_2(a) = diag(5, 5, 10) \tag{38}$$

3.4 The SDRE Controller Algorithm Calculation

A_1, $B_1(x)$, $Q_1(a)$, $R_1(a)$ and $A_2(x)$,B_2, $Q_2(a)$, $R_2(a)$ matrices are created for calculation. After that, they are transmitted to the algebraic Riccati equation (ARE) solver for each gain, depicted in Fig. 4. For this paper, one of the direct methods is used for solving the ARE. After ARE block, these gains are sent individually to the controller architecture. In the ARE block, computation continues during a simulation. Essentially, online calculation of ARE is computationally expensive and rigorous for every sample time.[23] However, 3 by 3 SDC matrices are not a burden for computation. For all gains (K_{T-1}, K_{T-2} and K_{R-2}), ARE calculation is performed. ARE algorithm is given in the following way:

Algorithm 1 On-line Algebraic Riccati Equation Solver.

Step 1 Set Hamiltonian (H) Matrix ($2nX2n$) with SDC ($A(x)$, $B(x)$) and Weight ($Q(a)$, $R(a)$) matrices
Step 2 Sort eigenvalue and eigenvector of the H Matrix
Step 3 Diagonalize the stable and unstable eigenvalues of the H Matrix
Step 4 Give an index to eigenvalues (stable eig.=-1, unstable eig=+1)
Step 5 Rearrange upper side of the diagonalized matrix with stable, lower side with unstable eigenvalues ($2nX2n$)
Step 6 Rearrange the eigenvectors of the H matrix with the same order stated in Step 5
Step 7 Find P matrix from the stable eigenvectors
Step 8 Find gains (K) from the P

At the same time, observability and controllability (with the help of the A and B matrices) are checked simultaneously. The controllability matrix is given by $C_k = [B_k \quad A_kB_k \quad A_k^2B_k]$, $k = T1, T2, R2$. If the rank of the C_k matrices are 3, the system is controllable. The observability matrix is given by $O_k = [C_k \quad C_kA_k \quad C_kA_k^2]^T$, $k = T1, T2, R2$. If the rank of the O_k matrices is "3", the system is observable. However, any rank value other than "3" means uncontrollability and unobservability. The solution for this problem is changing control law from SDRE algorithm to LQR. As a result, the function of the SDRE calculation for gains is terminated. The drawback of the SDRE controller can be abolished by this solution.

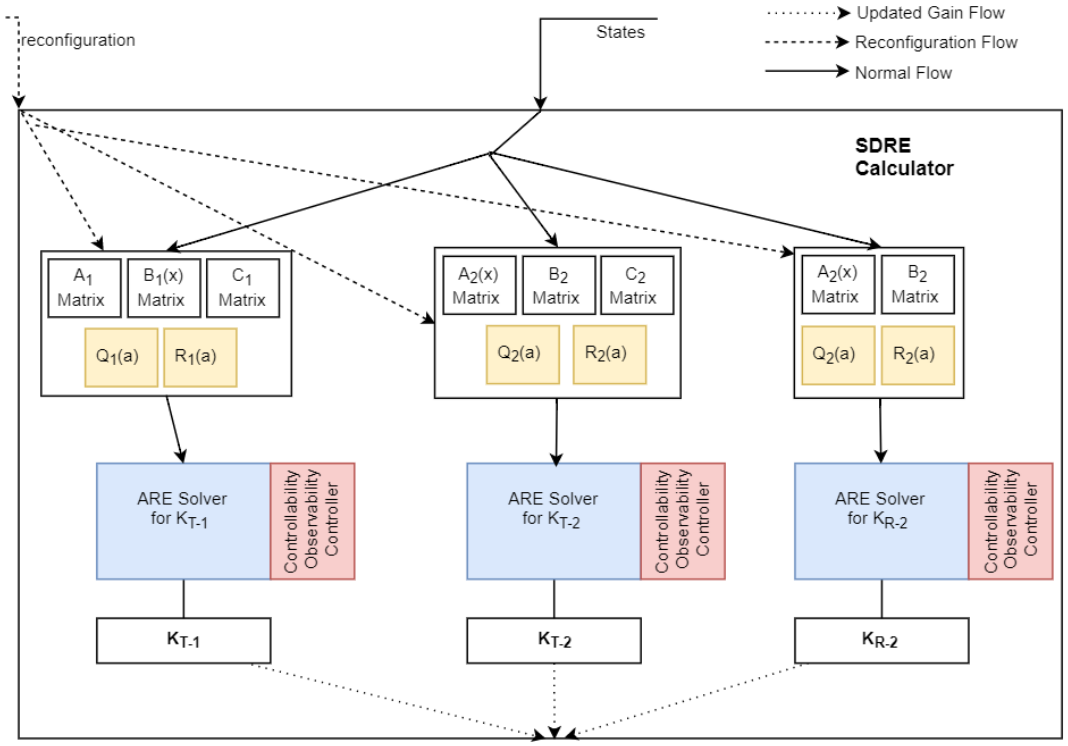

Figure 4: The SDRE algorithm calculation.

4. The Sensor: The SDRE Kalman Filter Algorithm Calculation

Nemra and Aouf[24] studied SDRE Nonlinear Filtering and compared the results with the Kalman Filter (KF) and Extended Kalman Filter (EKF). However, in this paper, the SDRE algorithm is used for filtering only Euler angles (ϕ, θ, ψ). Consider the nonlinear, continues, and stochastic system with dynamic model:

$$\dot{x}(t) = f(x) + B(x)u + B_w w \tag{39}$$

$$y(t) = Cx(t) + v \tag{40}$$

where, w and v are respectively process and measurement noise. Their uncorrelated covariances are Q_w and R_v.

For this system given in Equation 17, states (x) are ϕ, θ, ψ and inputs (u) are p, q, r. However, the SDC form can be given as $\dot{x} = A(\hat{x})u$ for computation:

$$\begin{bmatrix} \dot{\phi} \\ \dot{\theta} \\ \dot{\psi} \end{bmatrix} = \begin{bmatrix} 1 & \tan\theta\sin\phi & \tan\theta\cos\phi \\ 0 & \cos\phi & -\sin\phi \\ 0 & \frac{\sin\phi}{\cos\theta} & \frac{\cos\phi}{\cos\theta} \end{bmatrix} \begin{bmatrix} p \\ q \\ r \end{bmatrix} \tag{41}$$

After mathematical manipulation for optimal estimator, algebraic Riccati equations (ARE) is given by Khamis and Naidu:[25]

$$A(\hat{x})P + PA^T(\hat{x}) - PC^T R_v^{-1} CP + B_w Q_w B_w^T = 0 \tag{42}$$

and each sample time ARE is solved online. After that, P is found and used in K_{SDRE}. The error between y and $\hat{y}$ is multiplied by K_{SDRE}:

$$K_{SDRE} = PC^T R_v^{-1} \tag{43}$$

Finally, the estimated states ($\hat{\phi}$, $\hat{\theta}$, $\hat{\psi}$) are fed to the Flight Control Computer shown in Fig. 5.

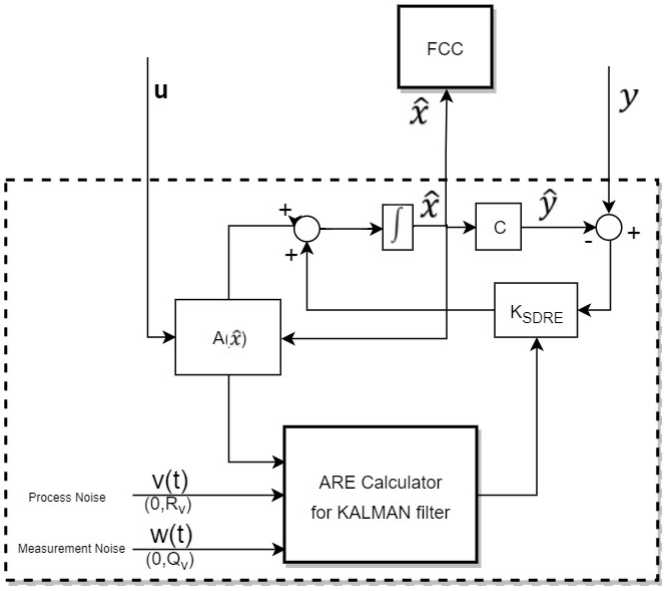

Figure 5: The SDRE Kalman Filter.

The filter is used for Euler angles. However, in Fig. 6, an example given for SDRE filtering for θ. In this figure, due to process and measurement noise, there is an oscillation from -1.2 to +1.2 degrees. With the help of the SDRE filter, this noise is filtered and θ is approximated to true value with an acceptable level.

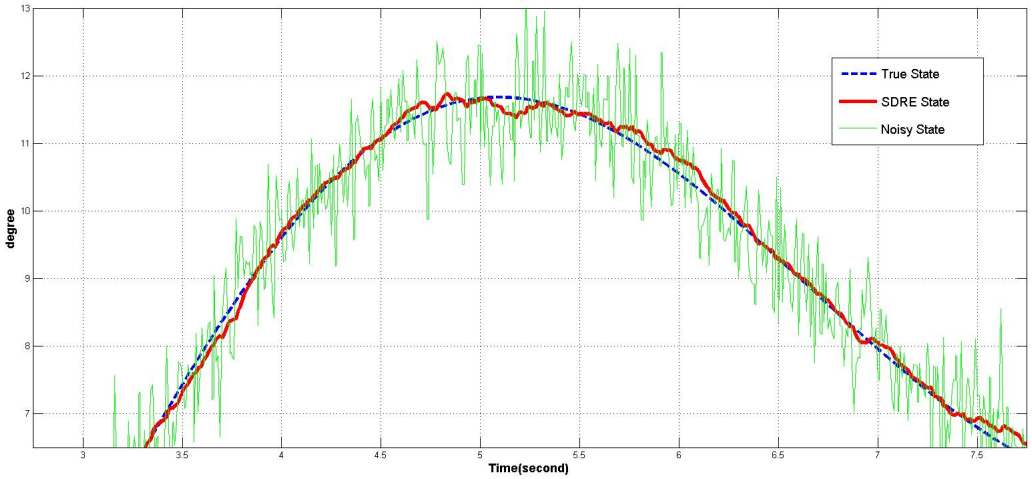

Figure 6: θ values

5. Atmospheric Environment: Turbulence Model

Dryden continues Turbulence model is used to simulate turbulence condition. For the specification, MIL-HDBK-1797 is preferred. Turbulence is a stochastic process. To define this process, turbulence intensity (σ), scale length (L) and airspeed (V) are used. The aircraft passes through turbulence with frequency (ω). Root-mean-square (RMS) values are the magnitude of the turbulence intensity (σ).

In accordance with the MIL-HDBK-1797, turbulence subdivided as low and medium/high altitude. W_{20} represents the wind speed at 20 ft. Typically, for light turbulence $W_{20} = 15$ knots, for moderate turbulence $W_{20} = 30$ knots, for severe turbulence $W_{20} = 45$ knots. Specifications for the low altitude model defined as equal to or less than 1000 ft are given:

$$2L_w = h \tag{44}$$

$$L_u = 2L_v = h/(0.177 + 0.000823 \times h)^{1.2} \tag{45}$$

$$\sigma_w = 0.1 \times W_{20} \tag{46}$$

$$\sigma_u = \sigma_v = \sigma_w/(0.177 + 0.000823 \times h)^{0.4} \tag{47}$$

Turbulence above 2000 ft is assumed to be isotropic. The turbulence intensity is a function of altitude and probability of exceedance of turbulence intensity. The RMS values of the turbulence intensity (σ) are given in Fig. 7. Specifications for the medium/high altitude model defined as equal to or higher than 2000 ft are given:

$$L_u = 2L_v = 2L_w = 1750ft \tag{48}$$

$$\sigma_u = \sigma_v = \sigma_w \tag{49}$$

The Dryden form of the power spectral density (PSD) for the turbulence velocities are represented as $\Phi_u(\omega)$, $\Phi_v(\omega)$, $\Phi_w(\omega)$ and for rates as $\Phi_p(\omega)$, $\Phi_q(\omega)$, $\Phi_r(\omega)$. As an example, power spectral density formula for vertical component of the velocity spectra:

$$\Phi_w(\omega) = \frac{2\sigma_w^2 L_w}{\pi V} \frac{1 + 12(L_w \frac{\omega}{V})^2}{(1 + 4(L_w \frac{\omega}{V})^2)^2} \tag{50}$$

In the model, filters are used to obtain turbulence wave. After finding turbulence intensity (RMS) values, this signal is passing from the filters with white noise. These low-pass filters (transfer functions) are derived from velocity and rates spectra. As an example, a filter for vertical velocity is given:

$$H_w(s) = \sigma_w \sqrt{\frac{2L_w}{\pi V}} \frac{1 + \frac{2\sqrt{3}L_w}{V} s}{(1 + \frac{2L_w}{V} s)^2} \tag{51}$$

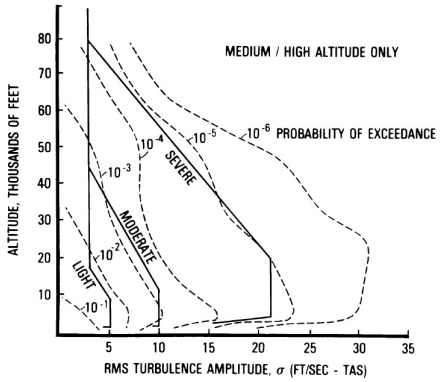

Figure 7: RMS values of turbulence intensity.

There are assumptions for the turbulence model. Thermal and mechanical turbulence due to terrain, wind shear and other meteorological phenomenon, lapse rates are not modelled.

6. The Reconfiguration Mechanism

SDRE algorithm is a nonlinear control algorithm, so it represents dynamics of the real system. In addition, another strongest characteristic of SDRE algorithm is designing flexibility of weight matrices. Without turbulence, the values of the Q and R matrices are given in Eq. (18), Eq. (19) and Eq. (37), Eq. (38). Several simulations show that these values are very useful for fault-tolerant capability. Namely, during recovery from control surface problems, these values are the best ones which were studied in another work. However, during turbulence condition, different Q and R matrices are transmitted to the SDRE control architecture in the flight control computer (FCC) block for K_{T-1}, K_{T-2} and K_{R-2}. For medium altitude (from $1000ft$ to $20\ 000ft$), these values are given in Table 2. These weight matrices are heuristically tuned with the result of the simulation. For tuning Q and R matrices, some basic rules are followed. Q is a weight matrix for states(for regulator)/errors(for tracker). Increasing its value is used to penalize from becoming too large. R is for input value and larger values are penalizing control action. Gains (K_{T2} and K_{R2}) to generate elevator and aileron command are tuned with Q and R values which is stated. To slow down these control surface movement, R values ($diag(50, 10, 10)$) can be increased. However, after several simulation tests, this solution can slow down the movement but it increases the g-force on the UAV. Finally, the best values are given in Table 2. For example, if the turbulence gets severe, these different $Q(a)$ and $R(a)$ values are transmitted to the controller to slow down the elevator and aileron movement with the help of stated gains. However, for rudder, the solution is increasing its movement. The idea for this solution is explained in results. During the online solution of the ARE, these different transmitted weight matrices are used. As a result, at medium and high altitude, deviation from the reference altitude is permitted with the help of the different $Q(a)$ and $R(a)$ values.

In the reconfiguration mechanism, there are interpolation tables using pre-lookup to define $Q(a)$ and $R(a)$ weight matrices for different turbulence conditions (light, moderate, severe) and different altitudes (low:under $1000ft$; medium: from $1000ft$ to $20\ 000ft$; high: from $20\ 000ft$ to $30\ 000ft$). In this paper, only turbulence is taking into account for Dryden turbulence model. For this model, RMS values shown in Fig. 7 are increased drastically from 1000 ft to 10 000 ft for severe turbulence. The same rising occurs but with different altitudes for other turbulence conditions. As a result, the main target area for reconfiguration is medium altitude because to reduce g-force, more slowing control surface movement is required.

Table 2: Values for SDRE gains in the Reconfiguration Mechanism for medium altitude.

	Q for K_{T1}	R for K_{T1}	Q for K_{T2} and K_{R2}	R for K_{T2} and K_{R2}
Normal	$diag(50, 50, 50)$	$diag(0.1, 0.1, 0.1)$	$diag(5, 5, 2)$	$diag(50, 10, 10)$
Light	$diag(40, 25, 50)$	$diag(0.1, 20, 0.1)$	$diag(10, 0.05, 7)$	$diag(50, 15, 10)$
Moderate	$diag(35, 15, 50)$	$diag(0.1, 17, 0.1)$	$diag(15, 0.15, 12)$	$diag(50, 10, 10)$
Mod. to Sev.	$diag(30, 5, 50)$	$diag(0.1, 14, 0.1)$	$diag(25, 0.4, 16)$	$diag(50, 10, 10)$
Severe	$diag(25, 3, 50)$	$diag(0.1, 12, 0.1)$	$diag(25, 0.5, 20)$	$diag(50, 10, 10)$

Also, as a measure, during unobservability and uncontrollability due to problem about the construction of the SDC matrices, reconfiguration mechanism changes the controller algorithm from SDRE to Linear Quadratic Regulator

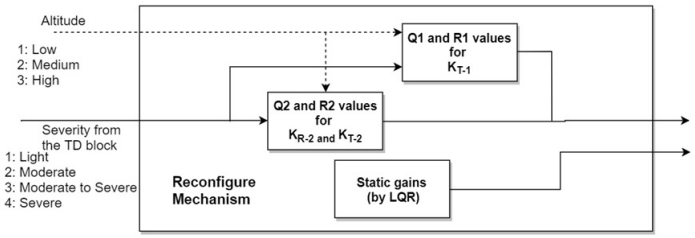

Figure 8: The reconfiguration mechanism.

(LQR). If unobservability and uncontrollability occur during calculation of the SDRE control gains, controller change from SDRE to LQR algorithm. Static gains are sent by the reconfiguration mechanism shown in Fig. 8 to the FCC shown in Fig. 3. Finally, SDRE controller becomes the LQR controller.

7. Results

For moderate and severe turbulence, there is a trade-off between achieving slower control surface movement and flying UAV safely. Because, if slower movement causes unstability, the result can be loss-of-control in-flight (LOC-I). As a result, the main objective is reducing g-force with the slower movement of control surfaces but not causes LOC-I.

7.1 First Scenario: Moderate to Severe Turbulence

In the first scenario, the altitude of the UAV is 8038 ft (2450 meter). At this altitude, RMS values for all turbulence severity, are approximately in the highest value shown in Fig. 7. Probability of exceedance of turbulence intensity value is taken 10^{-4} which represents moderate to severe turbulence. During 60 second simulation without reconfiguration of the controller, g-force is changing between -1.5 (from $+1$g) and $+1.7$ (from $+1$g) shown in the Fig. 9. However, if the reconfiguration occurs, g-force values are changing between -0.7 (from $+1$g) and $+0.7$ (from $+1$g).

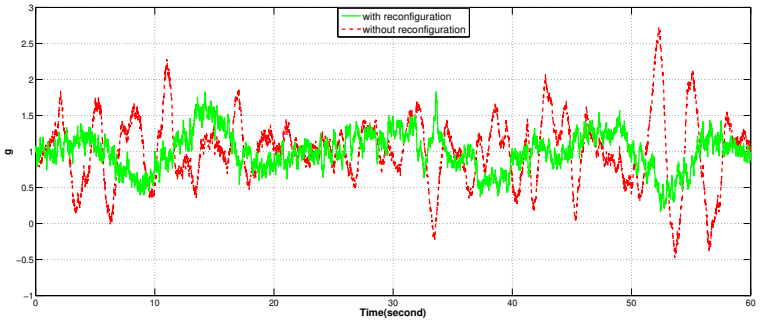

Figure 9: G-force during moderate to severe turbulence.

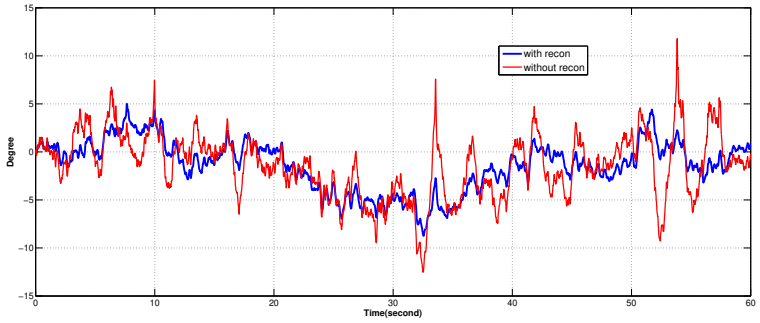

Figure 10: Elevator deflection during moderate to severe turbulence.

In Fig. 10, elevator movement is lessened with the help of the $Q(a)$ and $R(a)$ values which are sent by reconfiguration mechanism block. As a result, precise tracking performance is degraded for decreasing g-force. With the help of this, the frequency of the g-force is also decreased because the fast movement of the elevator for tracking command causes fluctuations in g-force.

In Fig. 11, normal tracking is shown. In these results, weight matrices (Q, R) given in Eq. (18), Eq. (19) and Eq. (37), Eq. (38) are used. Tracking performance for altitude is very good. However, this performance is not useful for reducing g-force on the body. Besides, there is an undesirable oscillation for ϕ and ψ.

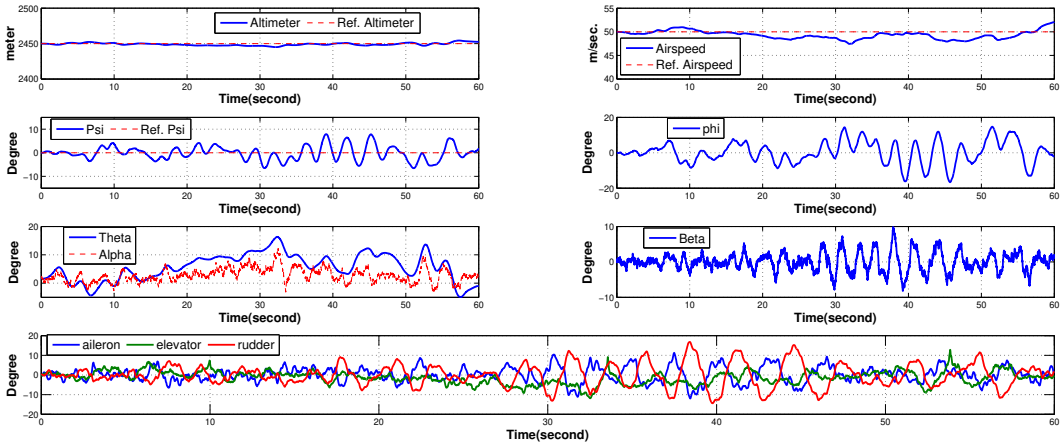

Figure 11: Medium altitude, moderate to severe turbulence without reconfiguration.

In Fig. 12, degraded tracking altitude performance is shown. As a golden rule for the flight in turbulent conditions, tracking performance can be degraded for decreasing g-force on the structure. Besides, the oscillation for ϕ and ψ is decreased. However, during several simulation tests, decreasing of the rudder movement range with the help of the reconfiguration induces ϕ, ψ and beta oscillation. As a result, the main idea for rudder reconfiguration is different from elevator reconfiguration so more movement range is required for the rudder. In the Fig. 12, rudder movement is maximum at 20 degrees. However, in Fig. 11, maximum value is 15 degrees.

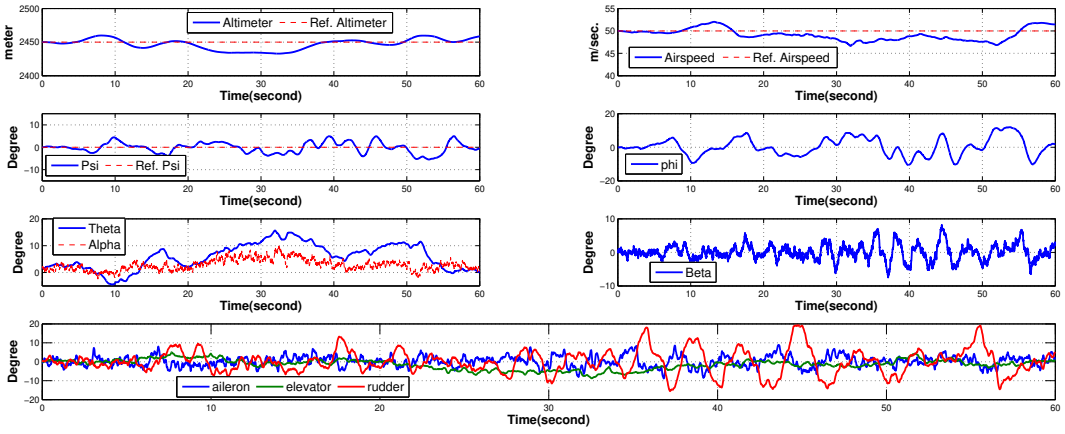

Figure 12: Medium altitude, moderate to severe turbulence with reconfiguration.

7.2 Second Scenario: Severe Turbulence

In the second scenario, the altitude of the UAV is 8038 ft (2450 meter). Probability of exceedance of turbulence intensity value is taken 10^{-5} which represents severe turbulence. If reconfiguration is not activated, after approximately

10 seconds, the result is LOC-I during severe turbulence. However, if different Q and R values given in Table 2 are sent by the reconfiguration mechanism, g-force is mitigated shown in Fig. 13. Maximum g-force for the without reconfiguration case before LOC-I approximately is -2.5 (from +1g). However, after reconfiguration, g-force is -0.5 (from +1g). As a result, the difference between these values is -2g. This significant value shows that reconfiguration can be useful during turbulence. Besides, unnecessary movement of the elevator is prevented shown in Fig. 14. As stated before, fluctuations in g-force are decreased. Above all, LOC-I is prevented after 10 seconds.

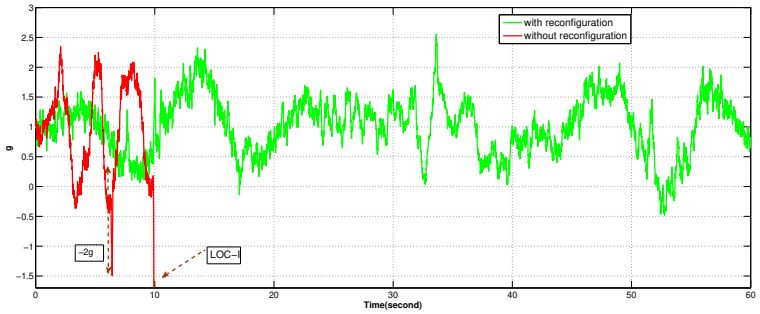

Figure 13: G-force during severe turbulence.

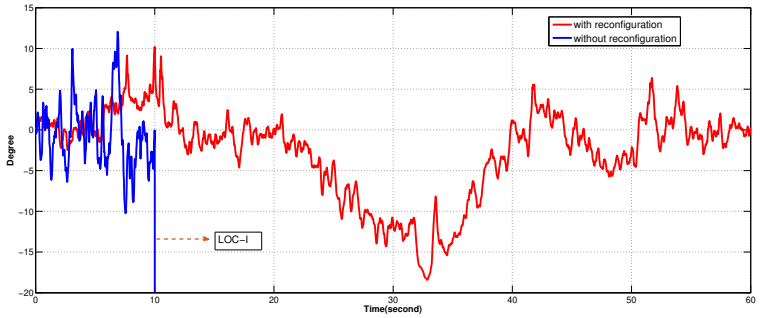

Figure 14: Elevator deflection during severe turbulence.

In the Fig. 15, the responses of the UAV is given. The altitude loss is -50 meter (approximately 164 ft) which is acceptable. The same reason stated in the first scenario, the movement of the rudder is required for preventing oscillation. As a result, the oscillation of the ϕ and ψ do not hinder flight safety with the help of the rudder.

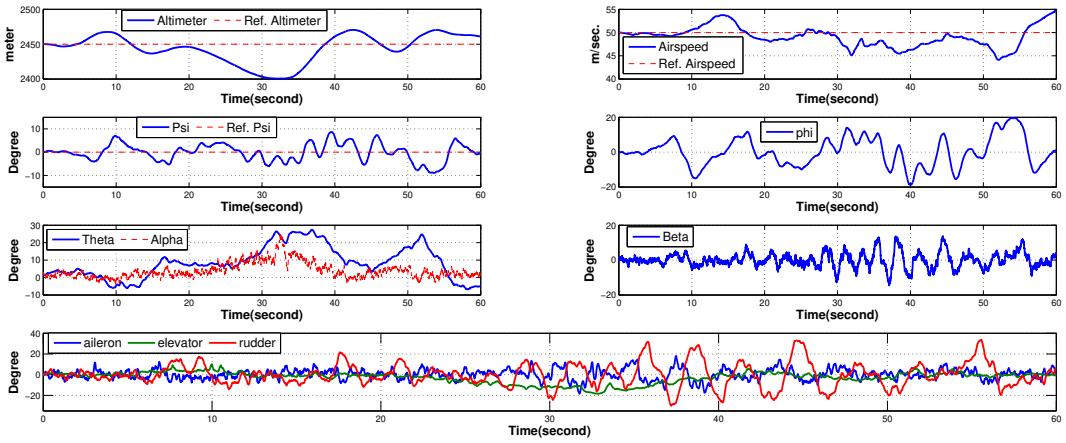

Figure 15: Medium altitude, severe turbulence with reconfiguration.

8. Conclusion

In this work, in order to improve flying qualities during turbulence, reconfigurable nonlinear SDRE controller is proposed. Normally, SDRE control algorithm is a nonlinear controller and can capture the nonlinearities in the system dynamics. Besides, with the help of the weight matrices, design flexibility can be achieved. Especially, during reconfiguration, the movement of the elevator and the tracking performance is decreased. The results presented in this paper indicate that g-force is reduced significantly. In addition, the aileron movement is decreased slightly. However, for preventing oscillation and LOC-I, rudder movement range is increased. For sensors, SDRE nonlinear filtering is used for Euler angles and the result shows that it is beneficial.

In this paper, the solution is not a gust load alleviation (GLA). The cheap and basic solution to mitigate turbulence is reconfiguring the controller for aircraft which have only 3 control surfaces (aileron, elevator, and rudder). In addition, as future work, this reconfiguration feature can be mixed with gust load alleviation for more than three control surfaced aircraft.

9. Acknowledgments

This work was partially supported by The Scientific And Technological Research Council Of Turkey (TÜBİTAK) through BİDEB 2224-A "Yurt Dışı Bilimsel Etkinliklere Katılımı Destekleme Programı " funds.

References

[1] J. K. Evans. An examination of aviation accidents associated with turbulence, wind shear and thunderstorm. *Analytical Mechanics Associates, Inc., Hampton, Virginia, NASA/CR2013-21798*, 2013.

[2] Boeing. *Flights of innovation: Proving readiness helps speed new technologies to market.* [online] https://www.boeing.com/features/innovation-quarterly/may2017/feature-technical-flights-of-innovation.page on January 2019.

[3] Jeppesen Inc. Jeppesen EASA ATPL Training-Meteorology. 2015.

[4] Oxford. Oxford Aviation Academy ATPL Ground Training Series-Meteorology. 2008.

[5] CAE SimuFlute. King Air 350 Cockpit Reference Handbook. 2008.

[6] Boeing. B737-6Q8/-7Q8/-8Q8 Flight Crew Operations Manual. 2005.

[7] Airbus. A318/A319/A320/A321 Flight Crew Operating Manual.

[8] G. Pacheco dos Santos, J. Balthazar, F. C. Janzen, R. T. Rocha, A. Nabarrete, and A. M. Tusset. Nonlinear dynamics and SDRE control applied to a high-performance aircraft in a longitudinal flight considering atmospheric turbulence in flight. *Journal of Sound and Vibration*, 08 2018.

[9] K. W. Iliff. Identification and stochastic control of an aircraft flying in turbulence. *Journal of Guidance, Control, and Dynamics*, 1(2):101–108, 1978.

[10] J. Steck, K. Rokhsaz, U. Pesonen, B. Singh, , and R. Chandramohan. Effect of turbulence on an adaptive dynamic inverse flight controller. *Infotech@Aerospace*, 2005.

[11] T. Yang and J. Juan. Aircraft landing control based on adaptive CMAC. *Procedia Engineering*, pages 791–796, 2009.

[12] A. Jafar, S. Fasih-UR-Rehman, S. Fazal-UR-Rehman, N. Ahmed, and M. U. Shehzad. A robust $\mathcal{H}_\infty$ control for unmanned aerial vehicle against atmospheric turbulence. *2nd International Conference on Robotics and Artificial Intelligence (ICRAI)*, pages 1–6, 2016.

[13] S. Miyagaki and S. Suzuki. Model predictive flight controller using prior air disturbance information obtained by doppler LIDAR. *Procedia Engineering*, 99:1049–1061, 2015.

[14] L. Wen, G. Tao, H. Yang, and Y. Zhang. Adaptive turbulence compensation for aircraft flight control. *IEEE Chinese Guidance, Navigation and Control Conference (CGNCC)*, pages 1612–1617, 2016.

[15] X. Liu, Q. Sun, and J.E. Cooper. LQG based model predictive control for gust load alleviation. *Aerospace Science and Technology*, 71:499–509, 2017.

[16] M. Sato. Gust alleviation flight controller using robust model predictive control. *In Proc. IFAC volumes*, 43(15):7–12, 2010.

[17] N. Aouf, B. Boulet, and R. Botez. $\mathcal{H}_2$ and $\mathcal{H}_\infty$ -optimal gust load alleviation for a flexible aircraft. *in Proc. American Control Conference*, 3:1872–1876, 2000.

[18] H. G. Giesseler, M. Kopf, P. Varutti, T. Faulwasser, and R. Findeisen. Model predictive control for gust load alleviation. *4th IFAC Nonlinear Model Predictive Control Conference*, pages 27–32, 2012.

[19] F. Fonte, S. Ricci, and P. Mantegazza. Gust load alleviation for a regional aircraft through a static output feedback. *Journal of Aircraft*, 52(5):1559–1574, 2015.

[20] X. Wang, E. Van Kampen, Q Chu, and R. De Breuker. Flexible aircraft gust load alleviation with incremental nonlinear dynamic inversion. *Journal of Guidance, Control, and Dynamics*, 0(0):1–18, 0.

[21] T. Çimen. State Dependent Riccati Equation (SDRE) control: A Survey. *in Proc. 17th IFAC World Congress*, pages 3761–3775, 2008.

[22] D.Subbaram Naidu. *Optimal Control System*. CRC press, 2003.

[23] P. K. Menon, T. Lam, L. S. Crawford, and V. H. L. Cheng. Real-time computational methods for SDRE nonlinear control of missiles. *Proceedings of the 2002 American Control Conference (IEEE Cat. No.CH37301)*, 1:232–237 vol.1, May 2002.

[24] A. Nemra and N. Aouf. Robust INS/GPS sensor fusion for UAV localization using SDRE nonlinear filtering. *IEEE Sensors Journal*, 10(4):789–798, April 2010.

[25] A. Khamis and D. S. Naidu. Nonlinear optimal tracking with incomplete state information using finite-horizon State Dependent Riccati Equation (SDRE). *2014 American Control Conference*, pages 2420–2425, June 2014.